Comparative Study in Removal of Methylene Blue Dye by Zinc Oxide Nanoparticles Synthesized by Chemical Precipitation and Green Chemistry

A thesis submitted in partial fulfilment of the requirements for the award of the degree of

Master of Technology in Material Engineering

Jadavpur University in the year 2022

By

Subhadip Jana

Examination Roll No.- M4MAT22006

Registration No.-154368 of 2020-2021

Under the supervision of

Dr. Sathi Banerjee

DEPARTMENT OF METALLURGICAL AND MATERIAL ENGINEERING,

JADAVPUR UNIVERSITY

KOLKATA-700032, WEST BENGAL

DEDICATED

TO MY BELOVED PARENTS

Certificate

This is to certify that the thesis entitled **"Comparative Study in Removal of Methylene Blue Dye by Zinc Oxide Nanoparticles Synthesized by Chemical Precipitation and Green Chemistry**" has been carried out by **Mr. Subhadip Jana (Examination Roll No: M4MAT22006 and Registration No. 154368 of 2020-2021)** under my guidance and supervision and accepted in partial fulfillment for the degree of Master of Technology in Material Engineering from Jadavpur University. To the best of our knowledge the content of this thesis or any parts thereof have not been previously submitted for the award of any degree or diploma.

Prof. Pravash Chandra Chakraborti

Head of the Department
Department of Metallurgical and Material Engineering
Jadavpur University
Kolkata-700032

Dr. Sathi Banerjee

Associate Professor
Department of Metallurgical and Material Engineering
Jadavpur University Kolkata-700032

Prof. Chandan Mazumdar

Dean
Faculty of Engineering and Technology
Jadavpur University
Kolkata-700032

Declaration of Originality and Compliance of Academic Ethics

I hereby declare that this thesis "**Comparative Study in Removal of Methylene Blue Dye by Zinc Oxide Nanoparticles Synthesized by Chemical Precipitation and Green Chemistry**" contains literature survey and original research work by the me, as a part of my M. Tech Degree in Material Engineering during the academic session 2020-2022. All information in this document has been obtained and presented in accordance with academic rules and ethical conduct. I also declare that, as required by this rules and conduct, I have fully cited and referred all material and results that are not original to this work.

Name: Subhadip Jana

Examination Roll Number- M4MAT22006

Registration No- 154368 of 2020-21

Place- Kolkata

Date- Signature

Certificate of Approval

The foregoing thesis is hereby approved as a creditable study of an engineering subject and presented in a manner satisfactory to warrant acceptance as a pre-requisite to the degree for which it has been submitted. It is understood that by this approval the undersigned does not necessarily endorse or approve any statement made, opinion expressed or conclusion drawn there in but approve the thesis only for which it is submitted.

Committee on final examination for the evaluation of the thesis

---

Signature of Examiners

Acknowledgement

I would like to take this opportunity to express my heartfelt gratitude to the people who supported me throughout this research project. I would like to express my sincere gratitude to my supervisor Dr. Sathi Banerjee, Associate Professor, Department of Metallurgical and Material Engineering, Jadavpur University for her continuous support in this study and research, for her patience, motivation, and immense knowledge. Her guidance helped me throughout my research tenure and writing of this thesis.

I am deeply indebted to Prof. Pravash Chandra Chakraborti, Head of the Department of Metallurgical & Material Engineering for permitting me to carry out my research work in this department. I am also grateful to him as he allowed me to conduct characterization in his lab.

I also deeply acknowledge the help and guidance from my senior Dr. Priyankari Bhattacharya, WOS -B (DST), Department of Metallurgical and Material Engineering, Jadavpur University throughout the tenure of my M. Tech project, and convey my heartfelt gratitude for her guidance and support. I acknowledge her immense knowledge in this field.

I also pay my indebt acknowledgement to my parents for providing me endless support, blessings and aspirations in each synergy of life. Finally, I take this occasion to thank all my classmates whose cooperative attitude helped me very much. I also like to acknowledge the cooperation of all the staff members of department for their support and help during my project work.

Everything in this nature is time bound, so thanks to ‘Almighty God’ for successful completion of the work in time.

Name- Subhadip Jana

Place- Kolkata

CONTENTS

Page No.

Certificate *ii*
Declaration of Originality and Compliance of Academic Ethics *iii*
Certificate of Approval *iv*
Acknowledgement *v*
Contents *vi-vii*
List of Figures *viii*
List of Tables *ix*
Abstract *x*

Chapter 1: INTRODUCTION 2-7

1.1 Nanotechnology

1.2 Classification of Nanomaterials

1.2.1 Metal Oxide Nanoparticles

1.3 Different synthesis methods for Metal Oxide Nanoparticles synthesis

1.3.1 Precipitation method
1.3.2 Plant mediated (green synthesis) method

Chapter 2: LITERATURE REVIEW 9-11

Chapter 3: MATERIALS AND METHODS 13-18

3.1 Materials and equipment used

3.2 Methodology

3.2.1 Synthesis of zinc oxide nanoparticles

3.2.1.1 Chemical route
3.2.1.2 Green route

3.2.2 Dye removal study

3.2.2.1 Preparation of Methylene blue dye
3.2.2.2 Equilibrium study
3.2.2.3 Kinetic study

Chapter 4: CHARACTERIZATION OF MATERIALS 20-24

4.1 XRD

4.2 FTIR

4.3 FESEM & EDS

4.4 TGA/DTA

4.5 UV Vis Spectrophotometer

Chapter 5: RESULTS AND DISCUSSION 26-38

5.1 Characterization ZnO NPs

5.1.1 XRD

5.1.2 FTIR

5.1.3 FESEM & EDS

5.1.4 TGA/DTA

5.2 Application of ZnO NPs in dye removal

5.2.1 Preparation of calibration curve

5.2.2 Adsorbent dose vs Removal

5.2.3 Initial dye concentration vs Removal

5.2.4 Contact time vs Removal

Chapter 6: CONCLUSION 40-41

REFERENCES 42-47

LIST OF FIGURES

Figure No.	Description	Page No.
Figure 1	Different synthesis routes of Metal oxide NPs	4
Figure 2	Top down and bottom-up approach	5
Figure 3	Graphical representation of Precipitation method	6
Figure 4	Steps involved in Precipitation synthesis	7
Figure 5	Spanish cherry (*Mimusops elengi*)	13
Figure 6	Synthesized ZnO NPs and dry leaf powder	16
Figure 7	ZnO NPs (Chemical route) before and after adsorption of dye	17
Figure 8	ZnO NPs (Green route) before and after adsorption of dye	17
Figure 9	Visual representation of dye removal study	18
Figure 10	SmartLab SE XRD set up	21
Figure 11	IRPrestige-21 FTIR Machine set up	22
Figure 12	FESEM & EDS set up	22
Figure 13	TG/DTA set up	23
Figure 14	UV Vis Set up	24
Figure 15	XRD of ZnO (Chemical synthesized)	26
Figure 16	XRD of ZnO (Green synthesized)	27
Figure 17	XRD of ZnO (Green synthesized calcined)	27
Figure 18	FTIR of ZnO NPs (chemical route)	29
Figure 19	FTIR of ZnO NPs (green route)	29
Figure 20	FTIR of dry leaf powder	30
Figure 21	FESEM images of ZnO NPs (Chemical precipitation method)	31
Figure 22	FESEM images of ZnO NPs (Green synthesis method)	31
Figure 23	FESEM images of ZnO NPs (Green calcined)	32
Figure 24	EDS of ZnO (Chemical route)	33
Figure 25	EDS of ZnO (Green route)	33
Figure 26	TGA/DTA plot of ZnO NPs (Chemical)	34
Figure 27	Calibration curve	35
Figure 28	Adsorbent dose vs Removal	36
Figure 29	Initial dye concentration vs Removal	37
Figure 30	Contact Time vs Removal	38

LIST OF TABLES

Table No.	Description	Page No.
Table 1	FTIR functional groups	28
Table 2	Crystallite size from XRD data	30

Abstract

Zinc Oxide nanoparticles (ZnO NPs) have incited a lot of interest among the researchers across the globe due to its unique and diverse properties. In the present study ZnO NPs were synthesized via simple chemical precipitation route from zinc sulphate solution using alkali (sodium hydroxide) as precursors for precipitation. ZnO NPs was also synthesized via green route using *Mimusops elengi* (Spanish cherry) leaf extract at room temperature. A part of the green synthesized nanoparticle was calcined at 250°C. NPs were characterized by X-ray diffraction (XRD), scanning electron microscopy (SEM), energy dispersive spectroscopy (EDS) and Thermal gravimetric/Differential thermal analysis (TG/DTA). Flake-like morphology of the NPs was confirmed from FESEM micrographs. Average crystallite size as calculated by using Scherrer's equation was in the range of 30.38nm to 32.59 nm. Dye removal efficiency of the NPs synthesized in different routes were studied and compared using methylene blue as a model dye. Maximum removal of 99.2% was obtained for calcined green synthesized NPs followed by green synthesized NPs i.e., 82.1% and 63.8% for NPs synthesized in chemical route after 120 mins of contact time using 10g/L dose, 30 ppm initial dye concentration and pH 7.

Keywords: *Nanoparticles, Zinc Oxide, Chemical precipitation, green synthesis, FTIR, XRD, FESEM, EDS, TG/DTA, Adsorption, Dye removal.*

Chapter 1

INTRODUCTION

Chapter 1

1.1 Nanotechnology

Nanotechnology is evolving as a state of art technology which has the potential to spark a new revolution in every field of science.[1] Nanotechnology can be identified as one of the challenging fields of recent research. It has become immensely popular among the researchers during the last few decades especially because of the unique, unusual and fascinating properties of nano sized particles, which can be used in a variety of applications, as opposed to their bulk counterparts. This technology incorporates 'research and technology ' development at the atomic, molecular or macromolecular levels. It deals with nanoparticles that are atomic or molecular aggregates characterized by the scale of approximately 1 to 100 nm in at least one dimension [2,3]. In accordance to the British Standards Institution [4], the definitions for the different relevant scientific terms that are being used are:

- Nanoscale: Approximate scale range of 1 to 1000 nm size.
- Nanoscience: It is the science that deals with the study of material at atomic, molecular and macromolecular scales and understanding their size and other structure-dependent properties and how the properties are different from those at bulk scale.
- Nanotechnology: It is a technology that involves design, characterization, production and application of structures, devices and systems by manipulating the size and shape of material on nanoscale dimension.
- Nanomaterial: Material with at least one dimension on the nanoscale (<100nm).
- Nano-object: Material possessing one or more dimensions at nanoscale level.
- Nanoparticle (NPs): Nano-object with three external nanoscale dimensions. Nanorod or nanoplate are the more convenient terms to be used in place of nanoparticle when the longest and the shortest axes lengths of a nano-object are different.
- Nanofiber: When two similar exterior dimensions are on nanoscale and a third larger dimension is present in a nanomaterial, it is called nanofiber.

Observation and manipulation of nanoscale materials have been made accessible since 1931, when Knoll and Ruska invented the electron microscope. The famous lecture (“There's Plenty of Room at the Bottom”) by Richard P. Feynman in 1959 [5] had greatly inspired upcoming research.

Nanotechnology has provided numerous innovative solutions in different fields of material science, biomedical, optics and electronics [6]. Nanotechnology provides a fundamental understanding of phenomena and materials at the nanoscale to create and use structures, devices, and systems that have novel properties and functions because of

their small and/or intermediate size. It has encouraged researchers and technologists to work in the field of nanotechnology from multidisciplinary directions, viz. Engineering, Biology, Physics and Chemistry. The application of active nanostructures and nano systems may bring significant changes in industry, agriculture, medicine, quality of life and most importantly the environment [7].

1.2 Classification of Nanomaterials

Nanomaterials (NM) can be both naturally occurred or man-made i.e., engineered nanomaterials. Based on the chemical composition engineered NMs can be classified broadly in three major groups:

- inorganic materials; such as metal NPs and quantum dots (QDs)
- organic NMs; such as carbon-based materials
- mixed organic– inorganic NMs, for example, gold NPs functionalized with cyclodextrins.

However, in general, five major groups are distinguished [8]:

- carbon NMs,
- metal oxide nanoparticles,
- zero-valence metal NPs,
- Quantum Dots
- dendrimers.

1.2.1 Metal Oxide Nanoparticles

Among different nanomaterials metal-oxide NPs are most important from their usage frequency [9]. In spite of long-term presence in the bulk form, nano-sized forms of titanium dioxide, alumina and iron oxides have entered the market recently and are being used in different consumer products. Zinc oxide (ZnO) and TiO2 are widely exploited due to their photolytic properties [10]. Nanoparticles like alumina (Al2O3) derivatives are applied in materials science (e.g., polymer composites and core–shell NPs for different applications, including catalysis [11], or to improve the mechanical characteristics of different materials), for example, use of Al2O3 NPs up to maximum replacement level of 2.0% in cement mortar produces concrete with improved split tensile strength [12].

ZnO also finds extensive applications in sunscreens, cosmetics and bottle coatings because of their ultraviolet blocking capability [13,14]. Other relevant metal-oxide NPs are based on cerium dioxide (CeO2,) chromium dioxide (CrO2) molybdenum trioxide (MoO3), bismuth trioxide (Bi2O3) and binary oxides {e.g., lithium-cobalt dioxide (LiCoO2) or indium-tin oxide (InSnO)} [15,16]. CeO2 is finding major uses as a combustion catalyst in diesel fuels to improve emission quality [17], and in solar cells, gas sensors, oxygen pumps, and metallurgical and glass or ceramic applications.

1.3 Different synthesis methods for Metal Oxide Nanoparticles synthesis

There are different synthesis routes available for synthesis of metal oxide nanoparticles. They can be mainly classified into three main types, viz.:

- Chemical synthesis.
- Physical synthesis.
- Biological synthesis.

A graphical representation of different available synthesis routes is shown below:

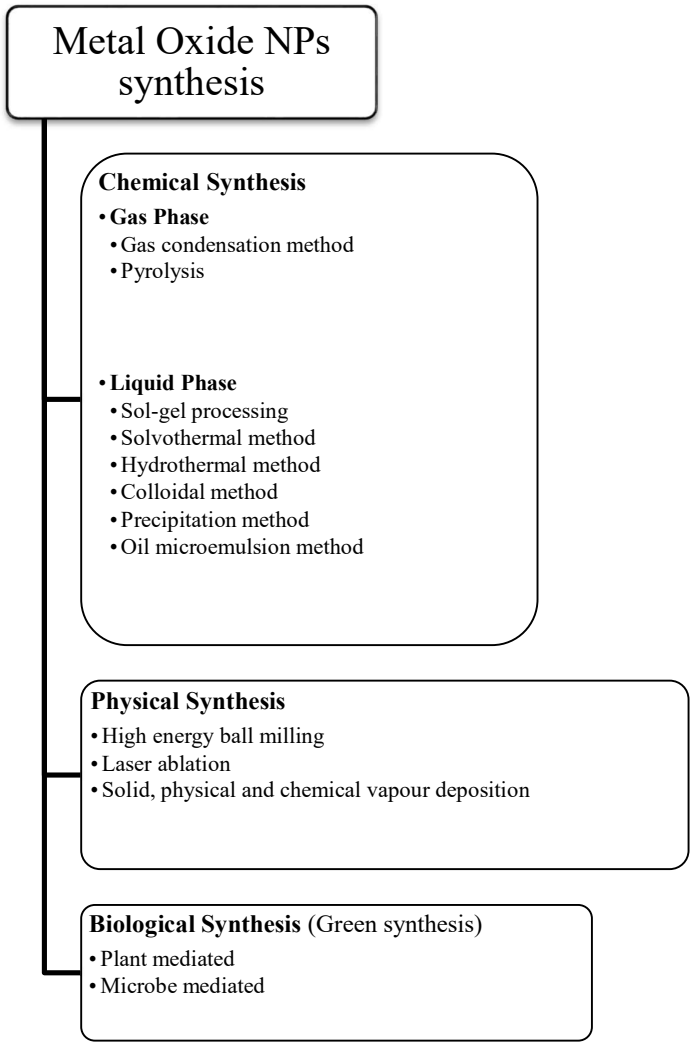

Figure 1: Different synthesis routes of Metal oxide NPs

Based on the starting phase of synthesis these routes can further be grouped into two methods:

- Top-down approach: Here bulk material is used as starting material for nanoparticle synthesis. These bulk materials are further processed to reduce its size up to nano size via different physical, chemical and mechanical processes. E.g. Mechanical milling (Ball milling, Mechanochemical method), Laser ablation, Sputtering.

- Bottom-up approach: Here the synthesis starts from atoms and molecules. E.g., Solid state methods (Physical vapour deposition Chemical vapour deposition), Liquid state synthesis methods (Sol gel methods Chemical reduction Hydrothermal method Solvothermal method), Gas phase methods (Spray pyrolysis Laser ablation Flame pyrolysis), Biological or green synthesis methods (Bacteria Fungus Yeast Algae Plant extract) and other methods like Electrodeposition process Microwave technique Supercritical fluid precipitation process Ultrasound technique.[18]

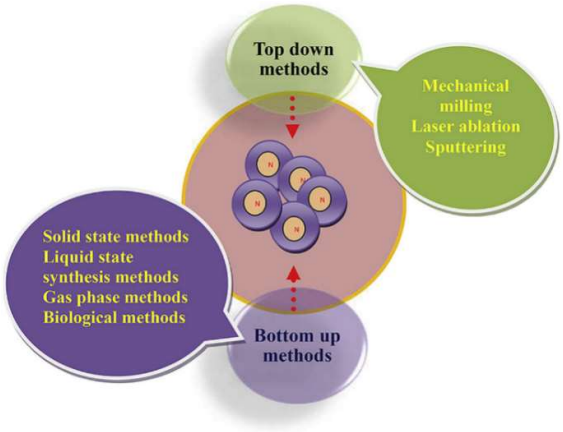

Figure 2: Top down and bottom-up approach

However, nanoparticles manufactured by physical methods usually require more control to obtain the desired shape and size [19]. Chemical parameters (e.g., pH, temperature, synthesis) can produce NPs with different desired properties. Size, shape and crystal structure of NPs, as well as composition (single or complex), determine their mobility, chemical and physical properties in different systems. Despite the fact that the majority of NPs are produced by physical methods such as arc discharge, evaporation, laser ablation, among others, chemical methods have demonstrated to be more effective in controlling size and shape [20]. Physical processes require high vacuum and they are energy consuming. Chemical methods such as precipitation, co-precipitation, solvothermal, sol–gel, sonochemical, spray pyrolysis, hydrothermal, and electrodeposition processes [21-25] have an advantage of being cost effective and they

are mass-production oriented. In contrast, their disadvantage lies in their uncongenial nature to the environment.

On other hand greener approaches are environmentally friendly and also easy to synthesis methods. Biosynthesis of nanoparticles using plant-based extracts is one such promising method. Indeed, this biosynthesis approach has been proved to be effective in the synthesis of metal oxide nanoparticles [26-28].

Zinc oxide nanoparticles like other metal oxide NPs can be synthesized via many of the above-mentioned synthesis routes. Looking at the above-mentioned advantages and disadvantages, **precipitation method** under chemical synthesis and plant mediated method under bio synthesis **(green synthesis)** are chosen as economic, scalable and sustainable options to synthesize Zinc Oxide NPs for the present study.

1.3.1 Precipitation method

This is a kind of **wet chemical process** or liquid phase synthesis.[29] This is a cost effective, scalable method without involving complicated equipment. In this method nanoparticles are precipitated in a controlled manner from precursors (mostly inorganic nitrate, chloride, sulphate, etc. salts that are dissolved in water or any other suitable medium to form a homogeneous solution with clusters of ions) by chemical reduction. After precipitation, the solid mass is collected, washed and gradually dried by heating to the boiling point of the medium.

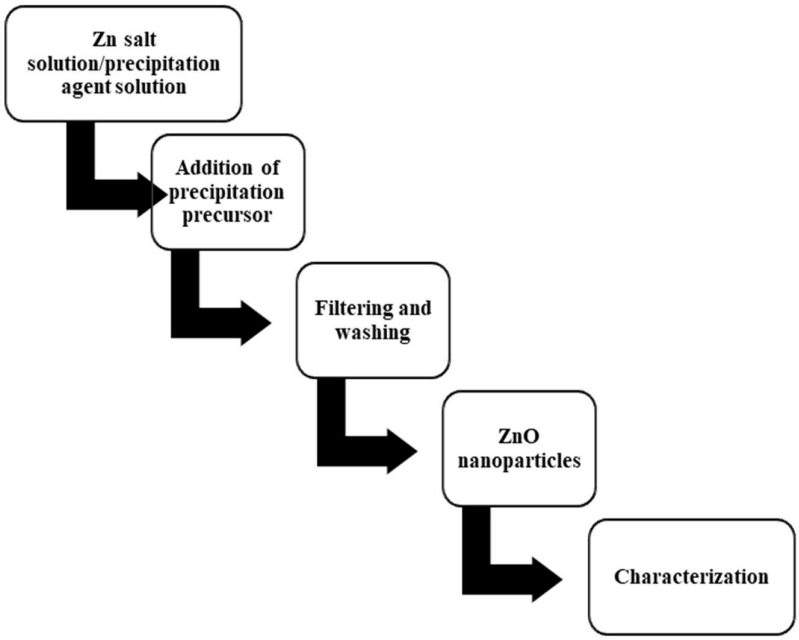

Figure 3: Graphical representation of Precipitation method

The three main steps involved in this synthesis method are:

- chemical reaction
- nucleation
- crystal growth.

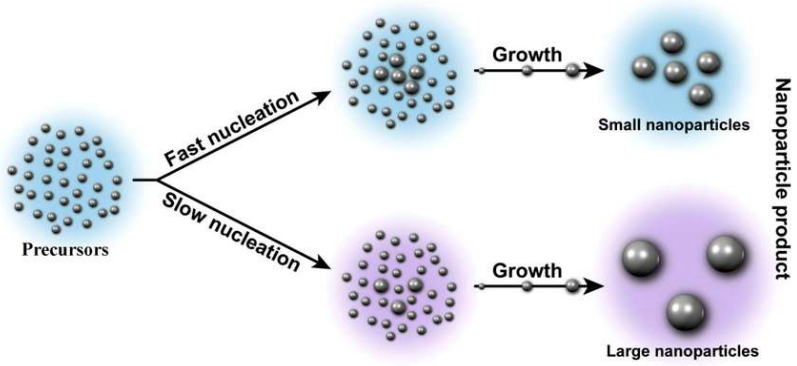

Figure 4: Steps involved in Precipitation synthesis

The crystal growth and their aggregation depend on many factors like the concentration of salt, temperature, the actual pH and the rate of pH change.

1.3.2 Plant mediated (green synthesis) method

This method comes under the biological synthesis method. Here degradation and metabolization of chemical substances are done by environmentally friendly biological processes. Here plants or plant parts are used to synthesise the NPs. In this case plant part (e.g., leaf) extracts are used as precursors instead of chemical agents. The green synthesis method employing biological plant extracts is one of the more extensively acknowledged routine due to its several advantages, such as requiring no additional chemicals, simple, environmentally friendly, inexpensive and reliable method. [30-39].

Chapter 2

LITERATURE REVIEW

Chapter 2

Given the possible technological usage of these substances, metal oxide nanoparticles represent a domain of materials chemistry that is of great interest. Research on creating synthetic routes to such nanostructures has been heavily influenced by the effects of these materials on industries like pharmaceutical, information technology, catalysis, energy storage, and sensing. In this review, advancements in traditional techniques to metal oxide nanoparticles as well as ventures into greener, gentler synthetic procedures were discussed. These novel methods could enable the energy-efficient synthesis of a wide range of metal oxide nanoparticles, whose resulting attributes can be exploited for usage in a variety of technologically significant domains. This is because the final particle structure and morphology are intimately linked to the synthetic pathway chosen. Additionally, we will give some examples of cutting-edge characterisation technologies that are assisting us in comprehending these structure-property-function correlations in metal oxides with such tiny size dimensions.

The surface, optical, thermal, and electrical properties of metal and metal oxide nanoparticles are among the many physicochemical traits that set them apart from their original bulk counterparts. Reducing or oxidising/precipitating agents are used while synthesising metal and metal oxide nanoparticles accordingly. [40]

AgNPs are gaining popularity due to their extensive use in a variety of products, including antimicrobial agents, food packaging materials, food storage containers, fabrics, room sprays, detergents, shampoo, soap, toothpaste, paint, waste water treatment and so on.[41]

Copper nanoparticles (Cu NP) are widely used in a variety of commercial applications, including antimicrobial agents, catalysts, gas sensors, electronics, batteries, heat transfer fluids etc. [42]

TiO2 nanoparticles are among the most widely used nanoparticles, with applications including cosmetic and skin care products, antibacterial and cleaning air products, paints, and organic matter decomposition in wastewater.[43] Several other nanoparticles are used in various industries to improve the quality of products and services. For example, Cerium dioxide nanoparticles (CeO2 NP) are primarily used in the automotive and semiconductor industries.

The citrate method is a traditional technique for creating gold nanoparticles. It is a very common technique; however, it once had a lot of problems, such stability and dispersity.

It's also known as the Turkevich approach. As time passed, new techniques for synthesis emerged. By using new techniques, the method of regulating the synthesis's

circumstances have produced outcomes that are better controlled in terms of size. [44]

The noble metal-incorporated materials are created using modified hydrothermal processes. Clusters of colloidal nanocrystals are typically produced by solvothermal techniques. This synthesis technique makes use of non-aqueous solutions. The benefit that is present on both the hydrothermal and sol-gel methods will be present in the product that is synthesized utilizing this process. [45-47]

Zinc oxide is an important functionalized metal oxide material due to its distinctive physical and chemical properties such as high chemical stability, high electrochemical coupling coefficient, broad range of radiation absorption, and high photostability. There are numerous methods for producing ZnO NPs, including vapor deposition, precipitation in water solution, hydrothermal synthesis, the sol-gel process, precipitation from microemulsions, and mechanochemical processes. This inspires the production of particles with varying shape, size, and spatial structure. [48] Controlled precipitation is a popular method for synthesising zinc oxide NPs because it yields NPs with repeatable properties.

Precipitated zinc oxide has also been reported to be obtained from aqueous solutions of zinc chloride and zinc acetate [49]. The concentration of the reagents, the rate of substrate addition, and the reaction temperature were all controlled parameters in this process. Zinc oxide with a monomodal particle size distribution and a high surface area was created.

A controlled precipitation method was reported by *Hong et. el* [50]. The process of precipitating zinc oxide was carried out using zinc acetate ($Zn(CH_3COO)_2 \cdot H_2O$) and ammonium carbonate ($(NH_4)_2CO_3$. These solutions were dosed into a vigorously mixed aqueous solution of poly(ethylene glycol) with an average molecular mass of 10,000. The resulting precipitate was calcined by two different methods. In the first, calcination at 450°C for 3 h produced ZnO labelled as “powder A”. In the second process, calcination took place following heterogeneous azeotropic distillation of the precursor; the resulting zinc oxide was labelled as “powder B”. Structural testing (XRD) and morphological analysis (TEM) showed that powder A contained particles with a diameter of 40 nm, while powder B contained particles with a diameter of 30 nm. Heterogeneous azeotropic distillation completely reduces the occurrence of agglomerates and decreases the ZnO particle size.

Kumari et al., (2015) studied influence of nitrogen doping on structural and optical properties of ZnO nano particles. Un-doped and N doped ZnO nano particles were synthesized by using chemical precipitation method. [51]

As reported by Ahmed et al., (2017) Mn-doped ZnO nano- powders have been

successfully prepared by a solid-state reaction route. [52]

The synthesis of ZnO nanoparticles in Sol-Gel route was explained by Rochman et al., (2017). The process parameters used were pH variation (in increasing order of 7to 12) in steps of 1 by using two principal reactions method to produce compound oxide, such as hydrolysis and condensation by considering Sodium hydroxide as an agent. Research reveals that the pH of the sol-gel will increase have a linear relation with the agglomeration of particle. [53]

The biological method of producing nanoparticles, also known as green synthesis or biosynthesis, employs microorganisms such as algae, fungi, yeast, bacterial, and plant extracts as the reducing agent. [54] Silver NPs were green synthesised (of size approx. 26 nm) successfully using *Nigella sativa* (black seed) aqueous extract and adsorption capacity for Indigo Carmine Dye Removal was studied. [55]

Datta et al. (2017) research investigated the potential of Parthenium hysterophorus leaf extracts for the extraction of zinc oxide nanoparticles with antimicrobial properties. Aqueous, methanolic, and ethanolic solutions were used to extract nanoparticles. UV-Vis spectroscopy was used to characterise the synthesised nanoparticles, with the maximum absorbance peak at 400 nm. The particles were spherical and cylindrical in shape, according to SEM and TEM analysis, with an average particle size ranging from 16 to 45 nm. [56]

Synthesis of zinc oxide nanoparticles (ZnO) by thermal method (under microwave irradiation) using tomato aqueous extract as a non-toxic and environmentally friendly reducing agent was investigated Sutradhar et al., (2016). They concluded that microwave-assisted green chemistry was used to create ZnO NPs. A simple method for producing large amounts of ZnO NPs with well-defined dimensions has been reported, using tomato extract as a reducing agent. This eliminated the need for toxic chemicals in nanoparticle production. The synthesis was carried out using a thermal process as well as microwave irradiation at various power levels, and the synthesised nanoparticles were successfully used to prepare nano-composites for photovoltaic applications. [57]

Though different synthesis methods and applications op ZnO NPs have been reported in the literature, but most of them were energy consuming. Also, very few studies were reported for the application of ZnO NPs in dye removal. These facts inspired the author to carry out the present study.

Chapter 3

MATERIALS AND METHODS

Chapter 3

3.1 MATERIALS AND EQUIPMENT USED

3.1.1 Chemicals

- Zinc Sulphate ($ZnSO_4.7H_2O$, GR, India)
- Sodium Hydroxide (NaOH, GR, India)
- Ethanol (CH_3CH_2OH, GR, India)
- Methylene blue ($C_{16}H_{18}ClN_3S$, GR, India)

3.1.2 Plant

- **General name:** Spanish cherry
- **Scientific name:** *Mimusops elengi*
- **Type of tree:** Medium sized Evergreen
- **Source of collection:** Jadavpur University campus

Figure 5: Spanish cherry *(Mimusops elengi)*

3.1.3 Apparatus

- Weighing Machine (Sartorius, Germany, 0.0001-220gm)
- Magnetic stirrer (Remi, India)
- Centrifuge machine (Tarsons, India)
- Hot air oven (G.B. Enterprise, India)
- Tube furnace (K. Furnace, India)
- Ultrabath Sonicator (PUS, India)

3.2 METHODOLOGY

ZnO NPs was synthesized by three routes viz. chemical precipitation method, green synthesis and calcination of green synthesized nanoparticles using zinc sulphate as precursors. The synthesized NPs were characterized in terms of XRD, FTIR, FESEM & EDS, and DGA/DTA. Methylene blue was taken as a model dye to evaluate the efficiency of synthesized ZnO NPs. The dye-removal capacity of ZnO NPs was measured using UV-Vis Spectroscopy and denoted by percent dye removal capacity of the synthesized ZnO NPs.

3.2.1 SYNTHESIS OF ZINC OXIDE NANOPARTICLES

3.2.1.1 Chemical route

3.2.1.1.1 Preparation of Precursors:

Zinc Sulphate heptahydrate ($ZnSO_4.7\ H_2O$) was taken as the precursor.

- Molecular weight of $ZnSO_4,7\ H_2O$ is: (65.38 + 32.065 + 15.9994*4 + 7*(1.00794*2 + 15.9994)) =287.54956 grams.
- To prepare 0.1M solution of $ZnSO_4.7\ H_2O$, 28.755 grams of $ZnSO_4.7\ H_2O$ (S) were weighed and dissolved in distilled (deionized) water. The solution was stirred with a stirring rod until it completely dissolved.
- The solution was then diluted with distilled water to get the final volume of 1000ml. Prepared zinc sulphate solution was kept in a glass container for further use.

Sodium Hydroxide (NaOH) solution acted as the precipitating agent in the synthesis of NPs. O.1N NaOH solution was prepared as follows.

1. Molecular weight of NaOH is (23+16+1) =40 grams.
2. 40 grams of sodium hydroxide pellets were weighed and dissolved in distilled (deionized) water. The solid was stirred with a stirring rod until it completely dissolved.
3. The solution was then diluted with distilled water to get the final volume of 1000ml and stirred again to get homogeneous. Prepared sodium hydroxide solution was kept in a glass container for further use.

3.2.1.1.2 Synthesis of nanoparticles:

- $ZnSO_4$ solution was taken in a 500 mL Erlenmeyer flask and was placed on a magnetic stirrer.
- NaOH solution was added dropwise in controlled manner in the $ZnSO_4$ solution

and stirred at 900 rpm using magnetic stirrer.

- The experiment was carried at room temperature (30±2 ℃)
- White precipitation occurred at around pH 8.2.
- After the precipitation settled over time, supernatant solution was discarded and the precipitate was collected and washed repeatedly with distilled water to remove any traces of alkali.
- The solution containing ZnO NPs was centrifuged and the NPs was collected.
- Collected ZnO NPs was dried in hot air oven.
- The resultant powder was collected and stored in desiccator for use in further study.

The chemical reaction involved here is:

$$ZnSO_4 + NaOH = ZnO \downarrow + Na_2SO_4 + H_2O$$

....Equation 1

3.2.1.2 Green route

3.2.1.2.1 Preparation of Precursors:

For green synthesis, *Mimusops elengi* leaf extract (along with small amounts of NaOH (0.1 N)) was used as precipitating agent.

- *Mimusops elengi* (Spanish cherry) leaves were collected and washed with distilled water many times to remove any surface dirt.
- Then the leaves were air dried followed by hot air oven-dried.
- Those dried leaves were boiled to extract all the phytochemicals (that would act as reducing agents).
- The extract was filtered using Whatman 42 filter paper and kept in for further use.

3.2.1.2.2 Synthesis of nanoparticles:

- $ZnSO_4$ solution (prepared as above) was taken in a 500 ml Erlenmeyer flask and was placed on a magnetic stirrer.
- Prepare leaf extract was added dropwise in a controlled manner in the ZnSO4 solution and stirred at 900 rpm.
- A small amount of 0.1N NaOH was also added to the solution.
- The experiment was carried out at room temperature (30+2 ℃)
- The solution turned into brownish from colourless.
- Brownish white precipitate was formed at around pH 8.
- After the precipitation settled over time, supernatant solution was discarded and the precipitate was collected and washed repeatedly with distilled water to remove any traces of alkali.

- The solution containing ZnO NPs was centrifuged and the NPs was collected.
- A part of it was dried in hot air oven and the other part was calcined in a tube furnace (JAY CRUCIBLES, India) at 250℃ for 10 mins.
- The resultant powder was stored and used for further study.

Figure 6: Synthesized ZnO NPs and dry leaf powder

3.2.2 DYE REMOVAL STUDY

3.2.2.1 Preparation of Methylene blue dye:

Methylene blue was taken as a model dye for the current study. A 100 ppm dye solution was prepared. 100mg of Methylene blue was weighed and added to 600ml distilled water and stirred. More distilled water was added to the solution and stirred to make a final solution volume of 1000ml.

This 100 ppm stock solution was further diluted to 50ppm which was diluted further to get 40ppm, 30ppm, 20ppm and 10ppm solution of dye.

3.2.2.2 Equilibrium Study:

100 ml of 30 ppm dye solution was taken in a 500 ml Erlenmeyer flask and 500 mg of ZnO NPs (Dose 5g/L) was added to the solution and kept for 24h. After that the solution was centrifuged and the supernatant was collected and analysed in UV-vis spectrophotometer.

The used adsorbent was collected for FESEM study.

Figure7: ZnO NPs (chemical route) before and after adsorption of dye

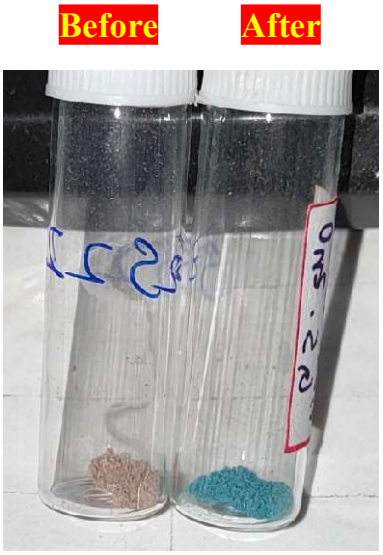

Figure 8 : ZnO NPs (green route) before and after adsorption of dye

3.2.2.3 Kinetic study:

To carryout kinetic study, required amount of model dye solution was taken in an Erlenmeyer flask and desired dose of ZnO NPs was added. The flask was placed on a magnetic stirrer to agitate the solution throughout the experiment at 1000 rpm.

Samples were taken at different time interval viz. 5, 10, 15, 30, 45, 60,75, 90,105, 120 mins and centrifuged to get the supernatant. Absorbance of those samples was measured by UV-Vis spectroscopy and respective concentrations were calculated using calibration curve. Those data were used to find out % dye removal capacity of ZnO NPs.

The procedure was carried out for different combinations of dose, contact time and initial dye concentration (in ppm) for a fixed pH value (pH 7).

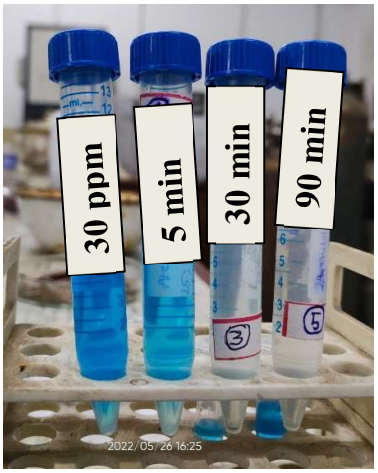

Figure 9: Visual representation of dye removal study

Chapter 4

CHARACTERIZATION OF MATERIALS

Chapter 4

The following characterization techniques were undertaken to understand the compound nature, morphology and purity of synthesized nanoparticles. The prepared sample was sonicated and characterized by using XRD, FTIR, FESEM & EDS and TGA/DTA.

4.1 XRD

X-Ray Diffraction is an important non-destructive technique in the characterization of nanoparticles. It is a rapid analytical technique that can provide information about crystalline nature, structure, and average size and is primarily used for the phase identification of crystalline materials.

The basis for X-ray diffraction analysis (XRD) is crystals' ability to diffract X-rays in a characteristic manner. Since a crystalline structure is periodic in nature, scattered radiation from these planes will be constructive or destructive. By analyzing the peak position in the diffraction pattern (using standard databases like Joint Committee on Powder Diffraction Standards or JCPDS) lattice parameters can be calculated and qualitative phase analysis can be done [59].

The geometrical interpretation of XRD phenomena is given by Bragg's law (by W.L. Bragg, 1913):

$$2D_{hk}\ sin\theta = n\lambda$$

....Equation 2

where, D_{hkl} = Lattice spacing(nm)
θ= Diffracted beam angle (in degree)
n= order of diffraction.

From XRD data crystallite size can be calculated by using Debye Scherrer equation.

Crystallite size, $d = k\lambda/\beta cos\theta$

where, d is the dimension(measured) of the particle in the direction perpendicular to the reflecting plane
k= Scherrer constant (crystallite shape factor with approximate value of 0.95),
λ= wavelength of the used X-ray beam (1.54184 Å or 0.154184nm),
β= Full width at half maximum (FWHM) of the peak in radian, and
θ= Bragg diffraction angle.

The XRD analysis for the present study was carried out in *SmartLabSE (Rigaku Corporation, Japan)* XRD machine. Scan parameters for the analysis were set to-

2θ range: 20-80°; Step: 0.01°; Scan Speed: 0.4°/ min;

Figure 10: SmartLab SE XRD set up

4.2 FTIR spectroscopy

Fourier Transform Infrared (FTIR) spectrometer, based on infrared spectroscopy, is an instrument for the characterization of unknown materials. During FTIR spectroscopy IR radiation is transmitted through the sample. The sample absorbs part of the infrared radiation, but some of it also passes through (transmitted). As a result, a spectrum is created that exhibits molecular absorption and transmission. Infrared spectroscopy probes the molecular vibrations. These vibrations are generally classified as stretching, bending, scissoring, rocking and twisting. Absorption bands corresponding to stretching have more amplitude than bending vibration. Identification of various functional groups can be done by these characteristic infrared absorption bands. The presence or absence of various chemical groups in a chemical structure can be confirmed using these absorption frequencies [58].

FTIR analysis in the present study was carried out in IRPrestige-21(Shimadzu, Japan). For FTIR analysis sample was mixed with KBr and a pellet was made by using hydraulic press. For baseline correction of the spectrum a KBr pellet was taken as a reference material. FTIR operation was carried out in 4000–400 cm^{-1} wavenumber range, in the absorbance mode. The absorbance data was transformed in to percentage transmittance using Beer-Lambert law.

Figure 11: IRPrestige-21 FTIR Machine set up

4.3 FESEM & EDS

Field emission scanning electron microscope (FESEM) is used to investigate the morphology (e.g., particle sizes and shapes), metallographic details, imperfections, and topology of nanocrystalline powders and bulk materials. A field-emission cathode in the electron gun of a scanning electron microscope provides narrower probing beams at low as well as high electron energy, resulting in both improved spatial resolution and minimized sample charging and damage. EDS (Energy dispersive spectroscopy) technique detects the chemical characterization and the elemental compositions of the sample in submicron scale.

The FESEM & EDS analysis for the present study was carried out in Inspect F50 (FEI, USA) FESEM machine. Gold coating was used for sample preparation for FESEM & EDS.

Figure 12: FESEM & EDS set up

4.4 TGA/DTA

Thermal gravimetric analysis (TGA) is a thermal analysis technique that measures changes in physical and chemical properties of materials as a function of increasing temperature (with constant heating rate) or time (with constant temperature and/or constant mass loss). TGA is done to determine specific properties of materials that display mass loss or gain owing to decomposition, oxidation, or volatile loss (such as moisture). In a TGA curve, the y-axis represents the percentage of mass loss and the x-axis represents temperature (or time, and most of the time a direct heating rate).
This technique has been used to characterize different metal oxide nanoparticles including ZnO NPs.

In DTA, the differential temperature change between the specimen and reference for a fixed amount of heat input is measured. Here, ΔT signal is referred to as the DTA signal. α-alumina is used as reference material in DTA. TGA-DTA techniques are preferably performed all together, in order to determine the range of thermal characteristics with a single sample run.
DTA is an important characterization tool to determine

- heat change measurements and whether the process and endothermic or exothermic.
- decomposition behaviour in various atmospheres.

The TGA/DTA analysis for the present study was carried out in EXSTAR 6000 TG/DTA 630(Seiko Instruments Inc., Japan) machine.

Figure 13: TG/DTA set up

4.5 UV Vis Spectrophotometer

Ultraviolet-visible (UV-Vis) spectroscopy is one of the most popular analytical techniques which is used to measure the maximum absorbance of a particle at a particular wavelength. Light is passed through a sample and the transmittance of light by a sample is measured. From the transmittance (T), the absorbance can be calculated as,

$$A = -log(T)$$

....Equation 3

UV spectroscopy obeys the Beer-Lambert law, which states that: when a beam of monochromatic light is passed through a solution of an absorbing substance, the rate of decrease of intensity of radiation with thickness of the absorbing solution is proportional to the incident radiation as well as the concentration of the solution.

The expression of Beer-Lambert law is-

$$A = log\,(I_0/I) = E.C.L$$

....Equation 4

Where, A = Absorbance

I_0 = Intensity of light incident upon sample cell

I = Intensity of light leaving sample cell

C = Molar concentration of solute

L = Length of sample cell (cm.)

E = Molar absorptivity

In the present study dye solution before and after adsorption (by ZnO NPs) was measured in UV Vis spectrophotometer (Shimadzu, UV 1800, Japan). The solution was centrifuged and supernatant was collected and subjected to UV analysis.

Figure 14: UV Vis set up

Chapter 5

RESULTS AND DISCUSSION

Chapter 5

5.3 CHARACTERIZATIONS ZNO NPs

Results of different characterization of ZnO NPs are discussed below.

5.3.1 XRD

XRD plots of synthesized ZnO NPs (Chemical, Green and Green Calcined) are shown in *Figure 15-17*. Presence of sharp peaks in the XRD plots indicated the crystalline nature of the synthesized compounds. The peaks, as observed in above XRD plots, was compared with available standards. It was found that peaks were in good agreement with the standard JCPDS card No. 36-1451. The peaks and its equivalent planes are shown in *Table 1*. The planes (100), (002), (101), (102), (110), (103), (112) and (202) corresponded to the hexagonal wurtzite structured ZnO crystals.

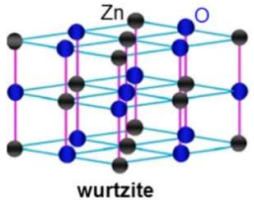

In XRD of chemically synthesized ZnO NPs, two peaks at 40.7°C and 59.4°C corresponding to $Zn(OH)_2$ (JCPDS card No. 76-1778) were observed. This showed that the synthesized nanoparticles contained some traces of unreacted zinc hydroxide as impurities.

.

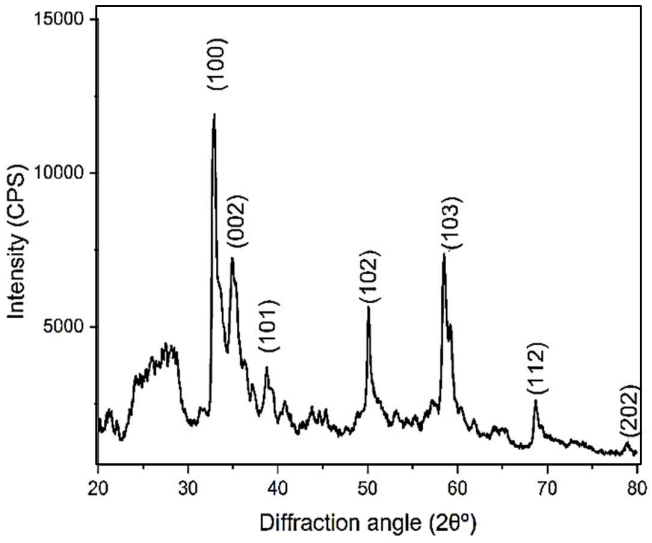

Figure 15: XRD of ZnO (chemical synthesized)

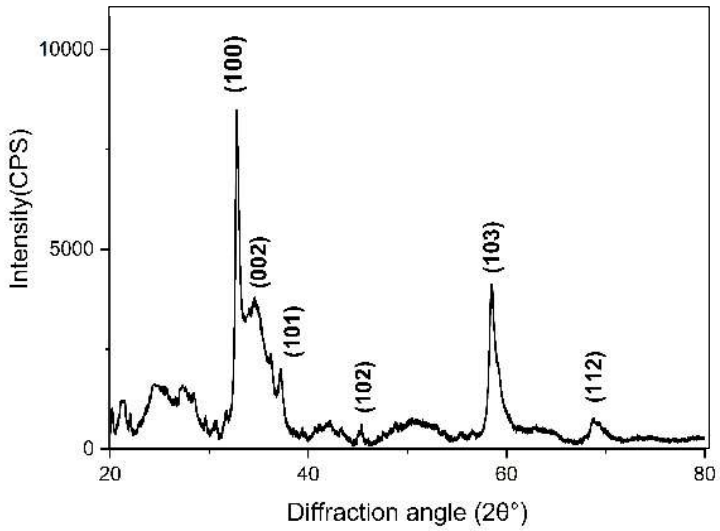

Figure 16: XRD of ZnO (green synthesized)

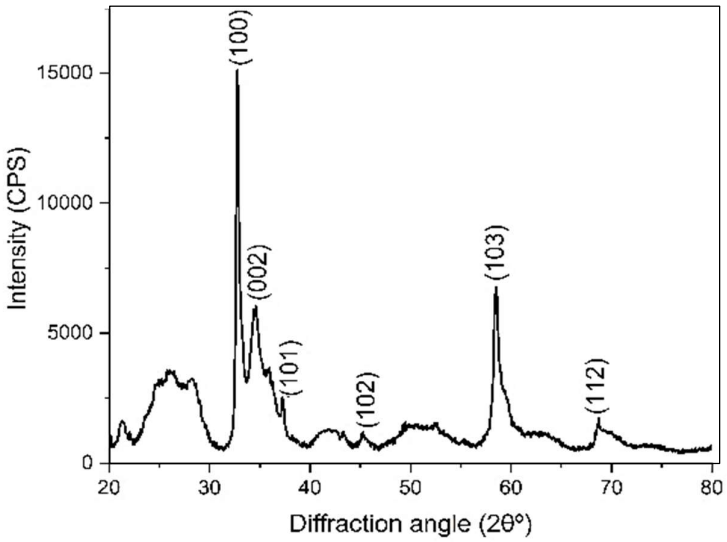

Figure 77: XRD of ZnO (green synthesized calcined)

The average crystallite size of synthesized ZnO NPs was calculated using Scherrer equation (*Table 1*). The average crystallite size for ZnO NPs synthesized via chemical route was 32.59nm whereas for green synthesized route the average crystallite size was calculated as 32.12nm. On the other hand, crystallite size reduced to 30.38nm after calcination of green synthesized ZnO NPs

Table 1: Crystalline size from XRD data

Angle,2θ(deg)	hkl	FWHM (deg) (β)	Size(nm)
ZnO Chemical			
32.94	100	0.54	28.28557
34.95	002	0.88	17.45023
38.75	101	0.35	44.36229
50.05	102	0.36	44.90277
58.5	103	0.53	31.67551
68.7	112	0.51	34.78723
78.9	202	0.71	26.71692
		Average	**32.59721 nm**
ZnO Green			
32.77	100	0.35	43.62151
34.6	002	0.71	21.60777
37.25	101	0.37	41.77561
45.3	102	0.54	29.39182
58.5	103	0.53	31.67551
68.75	112	0.72	24.6483
		Average	**32.12009 nm**
ZnO Green Calcined			
32.83	100	0.35	43.62823
34.61	002	0.54	28.41099
37.35	101	0.36	42.94869
45.36	102	0.53	29.95293
58.52	103	0.89	18.86479
68.78	112	0.96	18.48954
		Average	**30.38253 nm**

5.3.2 **FTIR**

FTIR of synthesized ZnO NPs synthesized via chemical and green route and dried *Mimusops elengi* leaves powder is shown in *Figure 18-20*. The absorbance bands of synthesized ZnO NPs, as observed in FTIR analysis are given in Table 2. The bands, observed between 880 and 650 cm^{-1}, could be due to the bending vibrational modes (wagging, twisting, and rocking) of coordinated water molecules.

The FTIR of plant extract (*Figure 20)* showed a broad peak range at 2994-3809 cm^{-1} which indicated the presence of various biological compounds like O-H, NH_2, H_3CO, HO-C=O and C=H aromatic stretching bonds of the various bioactive compounds. The

peak at 2060cm^{-1} corresponds to N=C=S stretching vibrations which could involve the thiamine based bioactive compounds. Comparing FTIR of leaf extract and green synthesized ZnO NPs, it might be inferred that the broad peak present in leaf became smaller and shifted towards lower wavenumbers 3400 cm^{-1} (NH, O-H stretching) after the synthesis of nanoparticles. Further it is noteworthy, that the phytochemicals like alkaloids, phenolic compounds and terpenoids etc. acted as reducing as well as stabilizing agent in synthesis of ZnO NPs.

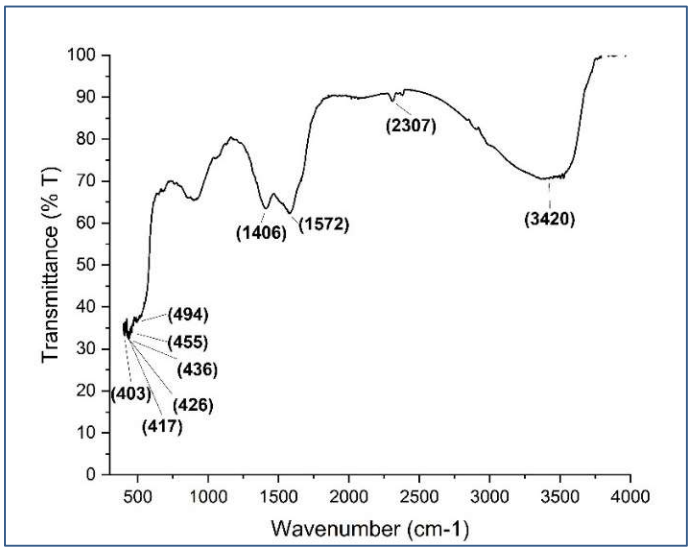

Figure 18: FTIR of ZnO NPs (chemical route)

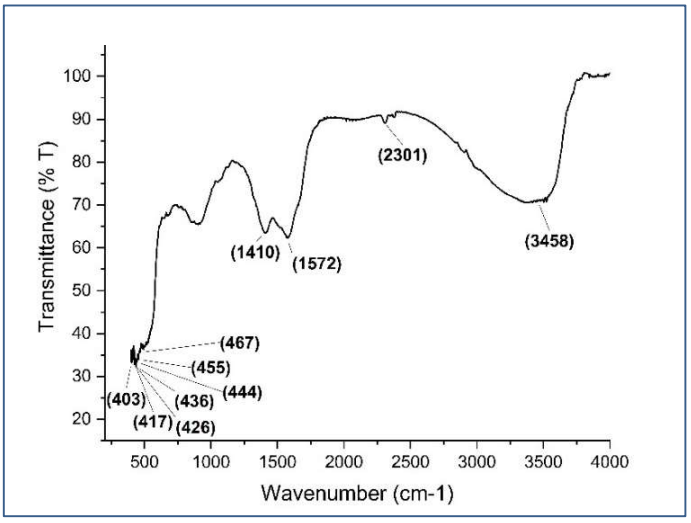

Figure19: FTIR of ZnO NPs (Green route)

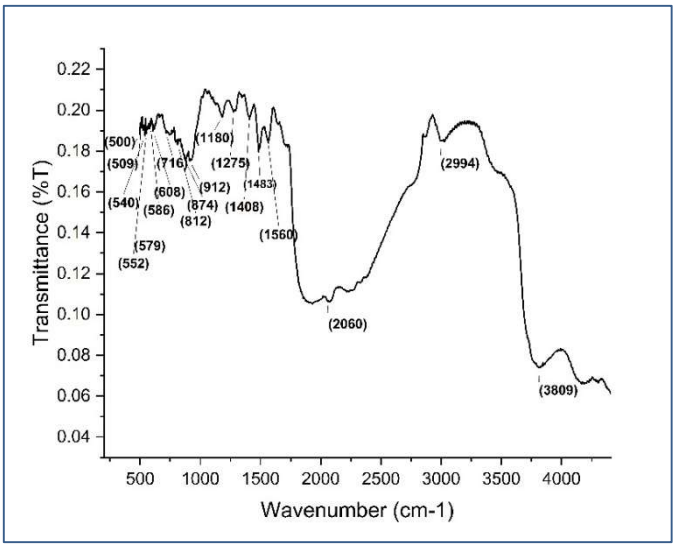

Figure 20: FTIR of dry leaf powder

Table 2: FTIR functional groups

	Peaks observed for ZnO NPs spectra	
Chemical precipitation method	**Wavenumber(cm^{-1})**	**Assignments**
	403,417,426,436,455, 494	Stretching of Zn-O
	1406	O-H bending vibration
	1572	C=C stretching
	2307	O=C=O stretching
	3420	H-O-H stretching vibration
Green synthesis method	403,417,426,436,444,455,467	Stretching of Zn-O
	1410	Phenolic O-H vibration
	1572	Alkaloid C–N stretching
	2301	O=C=O stretching
	3458	H-O-H stretching vibration

5.3.3 **FESEM & EDS**

The particle size and surface morphology of the synthesized NPs powder were examined using scanning electron microscope. SEM images of the synthesized ZnO NPs (chemical, green and green calcined) samples before and after adsorption of dye is depicted in *Figure 21-23*.

From the FESEM micrographs of the ZnO NPs it was observed that flake-like ZnO NPs was formed. Comparing FESEM images of NPs synthesised in different routes before and after adsorption (*Figure 21, Figure 22* and *Figure 23*), it was evident that, after adsorption of dye particles, the available sites on the surfaces of nanoparticles were greatly reduced. Moreover, in green synthesised ZnO NPs the surface morphology was seemed to be more uniform in nature providing more adsorption sites than that of NPs synthesized in chemical route. Surface morphology further improved by calcination which was evident from dye removal data where maximum adsorption occurred for calcined ZnO NPs synthesized in green route.

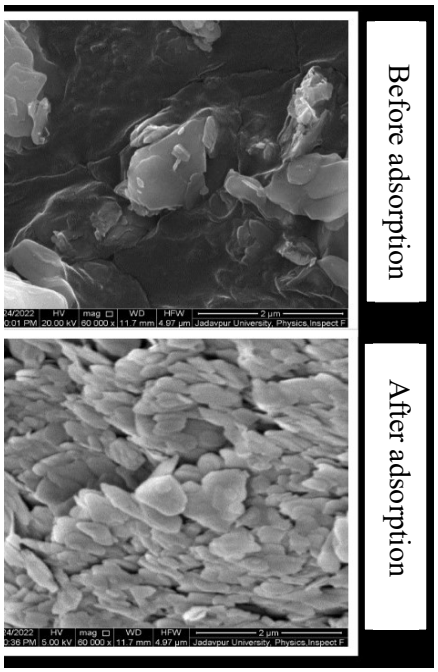

Figure 21: FESEM images of ZnO NPs (chemical precipitation method)

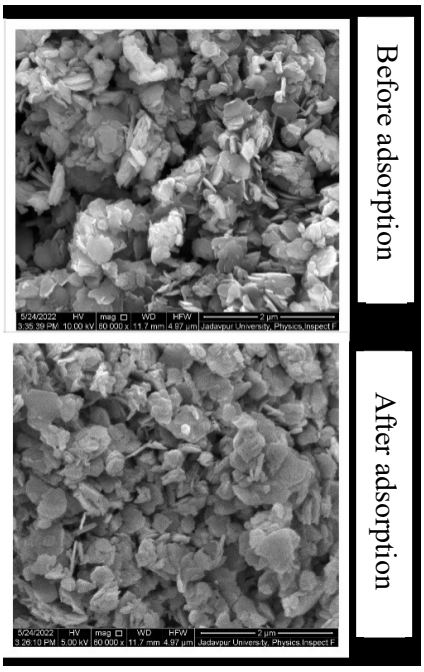

Figure 22: FESEM images of ZnO NPs (green synthesis method)

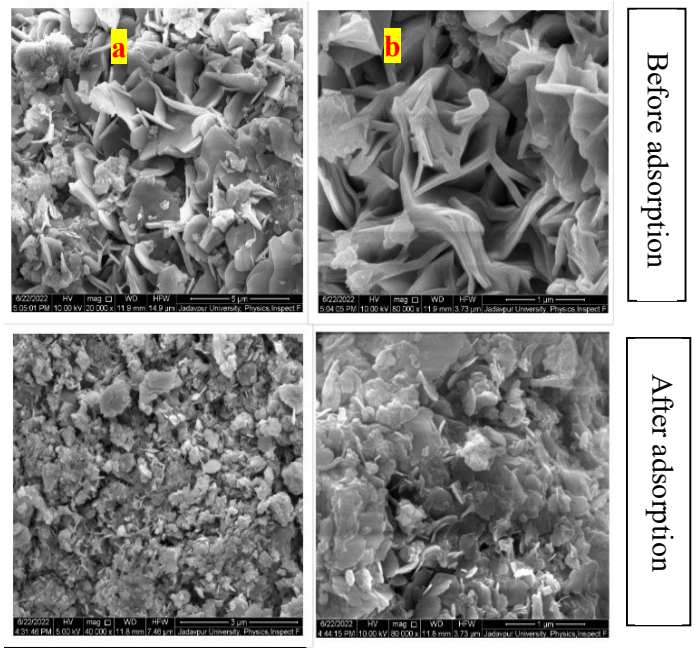

Figure 23: FESEM images of ZnO NPs (green calcined) at
a) 5µm scale and b) 1µm scale

Along with FESEM, EDS of synthesised NPs was also carried out to find the chemical characterization and elemental compositions of the samples. EDS analysis of the samples (chemical and green route) is shown in *Figure 24-25*.

The EDS spectrum of synthesized ZnO NPs (chemical route) (*Figure 24)* showed peaks of zinc (65.83%) and oxygen (26.94 %) elements which indicated that it contained ZnO with few peaks of sulphur (7.23%) as impurities.

EDS spectrum of green synthesized ZnO NPs (*Figure 25)* depicted three peaks, identified as zinc 80.34 % and oxygen 19.64 %, total 100 %, confirming ZnO NPs structure was composed of zinc and oxygen. The absence of any extra peak in EDS confirmed the formation of pure ZnO NPs in green route synthesis.

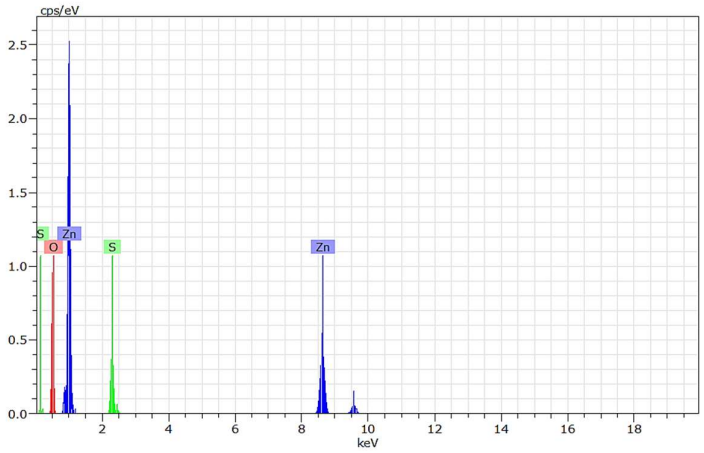

Figure 24: EDS of ZnO (Chemical route)

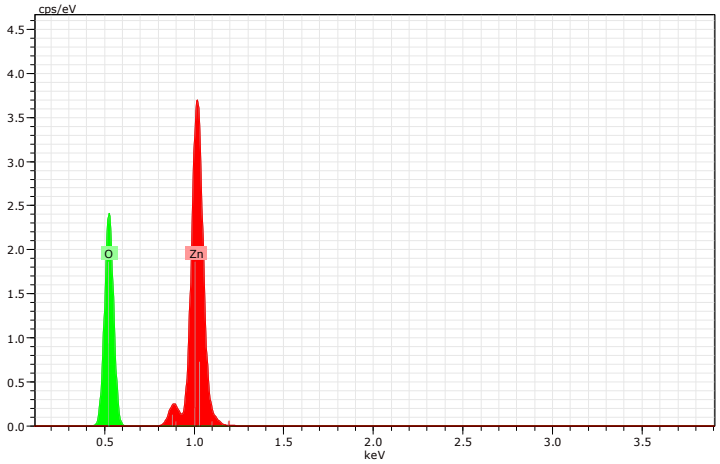

Figure 25: EDS of ZnO (Green route)

5.3.4 **TGA/DTA**

The sonicated sample was given for TGA/DTA analysis of the synthesised ZnO NPs (Chemical route). The plot is given in *Figure 26*. TGA plot can be analysed to get following information:

- The first weight loss of 17.50% in the temperature range 25°C -250°C can be assigned to desorption of chemically adsorbed water molecules on the ZnO NPs surfaces.

- Weight loss at around 250°C -300°C causing approximately 12.20 % loss in weight can be attributed to the loss of the other organic residues present in the sample. [60]
- 14.70% weight loss occurred at 700°C -780°C range. This weightlessness may be due to the decomposition of precursor used in the synthesis.
- No more weight loss is observed above 780°C, i.e., no decomposition or reaction occurs above this temperature point.

DTA plot can be analyzed to get following information:

- Two endothermic peaks can be found around 270°C and 780°C which are accompanied by weight losses. This endothermic effect may be the consequences of three processes: i) evaporation of adsorbed water molecules from the surface of ZnO NPs, ii) removal of organic contents and impurities from the lattice of the samples, and iii) conversion of $Zn(OH)_2$ into ZnO. [61].
- The peak (not sharp peak) observed around 40°C is due to the transition of ZnO nanoparticles.
- Exothermic peak observed in the range of 150°C to 200°C appears due to thermal lattice vibration.[62]
- Exothermic peak observed 700°C may appear due to combustion of resultant organics and by the crystallization of the ZnO powder.[62]

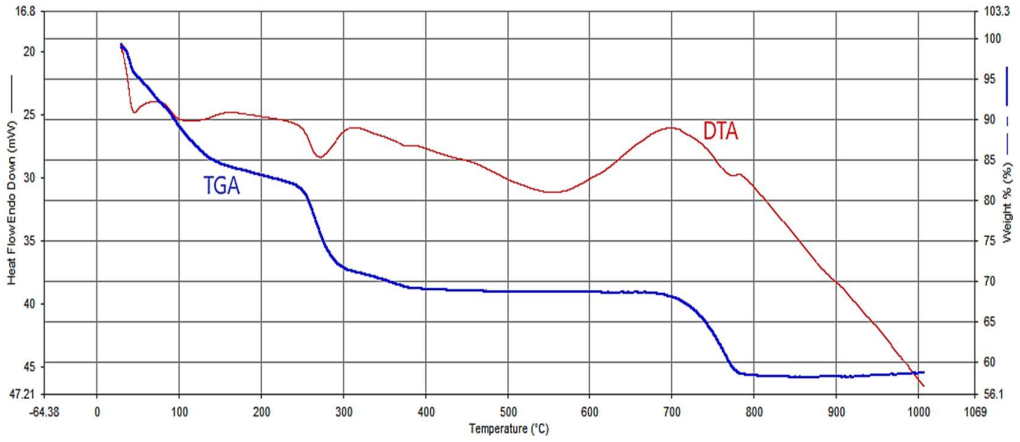

Figure 26: TGA/DTA plot of ZnO NPs (Chemical)

5.4 APPLICATION OF ZNO NPs IN DYE REMOVAL

5.4.1 Preparation of calibration curve

To observe dye removal efficiency of ZnO NPs, absorbance data obtained from UV Vis spectroscopy for methylene blue dye was used. λ_{max} for methylene was measured at 664nm. A calibration curve (*Figure 27)* was done using absorbance data of known concentrations (10, 20, 30, 40 and 50ppm). All the removal experiments were carried out in duplicate and the average value of each result was used for accuracy of the results.

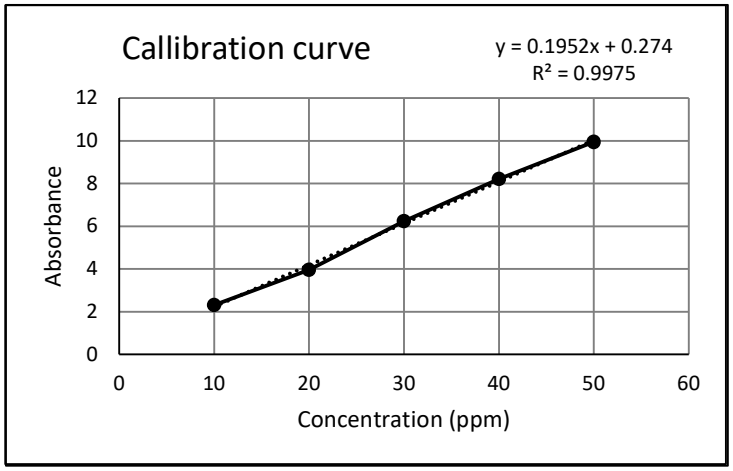

Figure 27: Calibration curve

Y-intercept and slope of the calibration line was noted and used to determine concentrations from absorbance data.

To determine the dye removal capacity of synthesized ZnO NPs, percentage removal was calculated using the following equation:

$$\%\ Removal = \left(\frac{C_o - C_t}{C_o}\right) \times 100$$

where, C_0 is the initial concentration of MB dye in ppm
C_t is the concentration of MB dye solution after adsorption in ppm.

Dependence of dye removal capacity (by synthesized ZnO NPs) on various factors like adsorbent dose, contact time and initial dye concentration (in ppm) were studied. Also, it was found from pH study (at pH 3, pH 5 and pH 7) that effect of pH is negligible in dye removal capacity. In fact, on acidic pH removal capacity decreased a little bit. Therefore, pH 7 had been chosen for further studies.

5.2.2. Adsorbent dose vs Removal

Figure 28 depicts the effect of adsorbent dose on the dye removal at an initial concentration of dye i.e., 30 ppm, contact time (120 mins) and pH 7. NPs dose used was varied from 1g/L-10g/L. It is observed that removal capacity of ZnO NPs increased with increasing NPs dose for all three synthesized ZnO NPs. Removal efficiency of about 61.54 %, 80.05% and 97.45% respectively was obtained at maximum NPs dose of 10g/L synthesized in chemical route, green synthesis and calcination of green synthesized NPs. The reason might be due to number of available adsorption sites increased with increasing adsorbent dose.

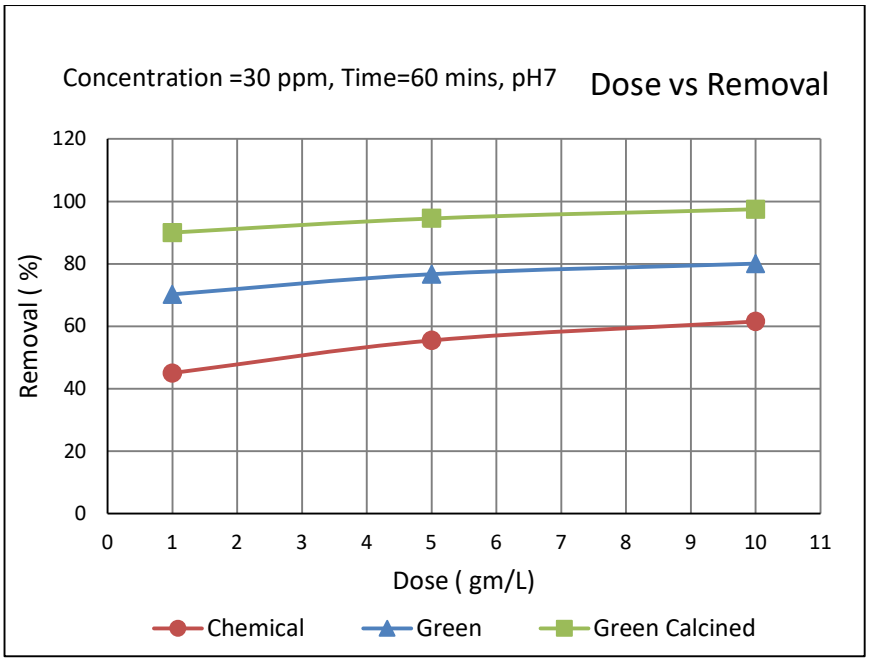

Figure 28: Adsorbent dose vs Removal

5.2.3. Initial dye concentration vs Removal

Effect of initial dye concentration on its removal can be observed in *Figure 29.* Initial dye concentration was varied from 10-50 ppm at a particular nanoparticle dose i.e., 10g/L, contact time (60 mins) and pH 7. Dye removal capacity of NPs decreased as initial concentration of dye increased. As evident from figure removal efficiency of 73.46%, 91.34% and 100% was obtained for NPs synthesized in chemical route, green synthesis and calcination of green synthesized NPs respectively at 10 ppm initial dye concentration. Removal efficiency on the other hand reduced to 34.25%, 56.78% and 80% respectively for initial dye concentration of 50 ppm. As dye concentration

increased available sites got exhausted and no further adsorption could occur at the particular dose.

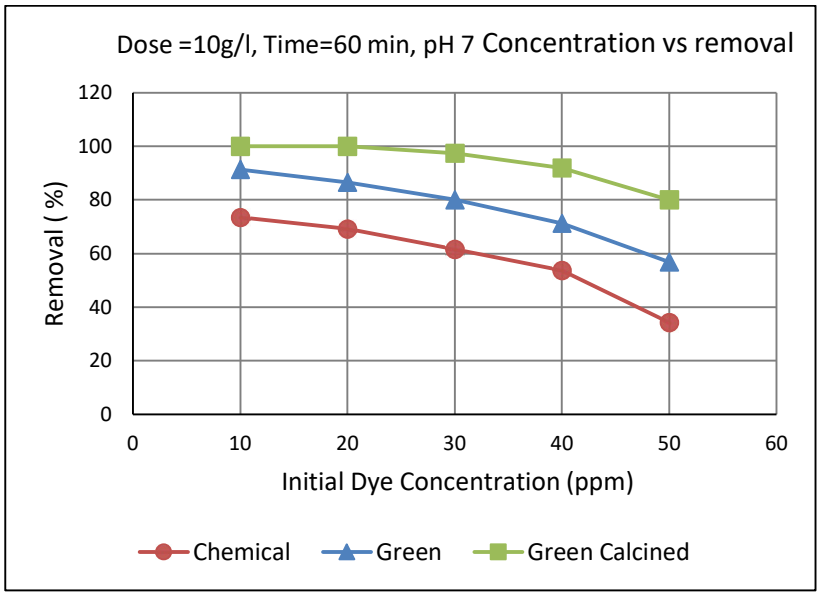

Figure 29: Initial dye concentration vs Removal

5.2.4. Contact time vs Removal

As shown in *Figure 30*, for a fixed nanoparticle dose of 10 g/L and initial dye concentration of 30ppm, removal of dye increased with increase in contact time. Removal efficiency of 61.54%, 80.05% and 97.45% was obtained at 60 mins of contact time for NPs synthesized in chemical route, green synthesis and calcination of green synthesized NPs respectively. This increased to 63.8%, 82.1% and 99.2% after 120 mins of contact time for NPs synthesized in chemical route, green synthesis and calcination of green synthesized NPs respectively. The resultant equilibrium time was found to be 90 mins. This might be attributed to the fact that attachment of more dye particles became available for binding on nanoparticles surface. But after a certain time, equilibrium was reached as with increase in time all available adsorption sites were occupied by the dye particles.

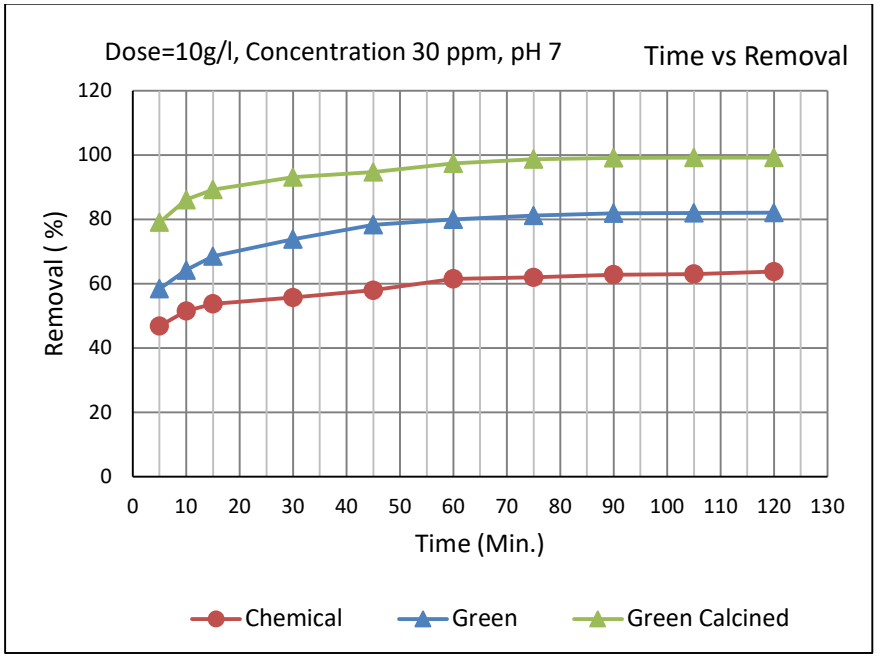

Figure 30: Contact Time vs Removal

From the above results, it is evident that green synthesized NPs as well as green synthesized NPs after calcination was more efficient in removal of dye from synthetic solution than chemically synthesized ZnO NPs. Phytochemicals, flavonoids, alkaloids etc. present in leaf extract (also confirmed in FTIR) provides an added advantage that helps in complete reduction of $Zn(OH)_2$ into ZnO. These phytochemicals might further take part in adsorption process thereby enhancing removal efficiency. On the other hand, in chemical precipitation few impurities, unreacted $Zn(OH)_2$, agglomerations were present which reduced its available adsorption sites. Since, the chemical precipitation method was carried out at room temperature, that might have some effect on the exposed surface area of NPs.

Calcined green synthesized NPs was seen to have more dye removal capacity (i.e., more available adsorption sites) than non- calcined green synthesized or chemically synthesized NPs. This might be due to the fact that after calcination the orientation of NPs became more regular with flake like structure thereby exposing more available adsorption site.

Chapter 6

CONCLUSION

Chapter 6

CONCLUSION

The following conclusions can be drawn.

1. Dye removal capacity of ZnO NPs was examined in the present study. Methylene blue was used as model dye.
2. Zinc oxide nanoparticles were synthesized by three route viz. chemical route, green chemistry and calcined of green synthesized nanoparticles.
3. XRD analysis of synthesized ZnO NPs showed sharp peaks corresponding to planes 100), (002), (101), (102), (110), (103), (112) and (202) confors the pure hexagonal wurtzite crystal structures of ZnO. Average crystallite size (calculated by Scherrer's equation) of ZnO NPs synthesized in chemical precipitation route was found to be 32.59 nm and that for green synthesized and green calcined were 32.12nm and 30.38 nm respectively.
4. The vibrational properties of the ZnO NPs were confirmed by FTIR. In FTIR spectrum of green synthesized ZnO, the presence of phytochemical group was also confirmed.
5. FESEM images revealed flake-like structure of synthesized NPs whereas EDS confirmed the chemical composition of ZnO as pure in green synthesized NPs and with few impurities of sulphur in chemically synthesized NPs.
6. The effect of adsorbent dose, initial dye concentration and contact time on the efficiency of removal of dye by ZnO NPs (prepared via and green chemistry) was investigated.
7. For a fixed nanoparticle dose of 10 g/L and initial dye concentration of 30ppm, removal of dye increased with increase in contact time. Removal efficiency of 61.54%, 80.05% and 97.45% was obtained at 60 mins of contact Dye removal capacity of green synthesized ZnO NPs was more than its chemical counterpart. One cause might be the presence of organic functional groups as confirmed by FTIR. Calcination improved the dye removal capacity further (might be due to more uniformity in particle orientation and modification in functional groups present in ZnO NPs).
8. Zinc oxide nanoparticles had been proved to an efficient material to remove methylene blue dye from synthetic solution.

FUTURE SCOPE

Application in real field textile industry wastewater will be conducted. The synthesized nanoparticle can be further characterized by TEM analysis for direct measurement of nanoparticle size, grain size, size distribution, and morphology. BET analysis can be performed to get specific surface area and porosity distribution of the synthesized NPs. Further, adsorption modelling can predict the adsorption isotherm for the kinetic study and adsorption capacity of produced nanoparticles. Also, Response Surface Methodology (RSM) can be applied to get relations between experimental and theoretical parameters related to dye removal study.

References

[1] C. M. Rico, S. Majumdar, M. Duarte-Gardea, J. R. Peralta-Videa, and J. L. Gardea-Torresdey, "Interaction of nanoparticles with edible plants and their possible implications in the food chain," Journal of Agricultural and Food Chemistry, vol. 59, no. 8, pp. 3485–3498, 2011.

[2] M.-C. Daniel and D. Astruc, "Gold nanoparticles: assembly, supramolecular chemistry, quantum-size-related properties, and applications toward biology, catalysis, and nanotechnology," Chemical Reviews, vol. 104, no. 1, pp. 293–346, 2004.

[3] H. Kato, "In vitro assays: tracking nanoparticles inside cells," Nature Nanotechnology, vol. 6, no. 3, pp. 139–140, 2011.

[4] ISO/TS 80004-1:2010, Nanotechnology – Vocabulary – Part 1: Core Terms. International Organisation for Standardisation: Geneva, Switzerland, 2010; https://www.iso.org/standard/51240.html (accessed July 17, 2017).

[5] Feynman RP. There's Plenty of Room at the Bottom. Eng Sci 1960; 23:22–36.

[6] Sanchez F, Sobolev K. Nanotechnology in Concrete—A Review, Construct Build Mater 2010;24:2060–71

[7] Fulekar. M.H., Nanotechnology Importance and Applications, I.K. International Publishing House, 2010.

[8] MarinellaFarré, Damià Barceló (2012). Chapter 1 - Introduction to the Analysis and Risk of Nanomaterials in Environmental and Food Samples. Spain: doi: https://doi.org/10.1016/B978-0-444-56328-6.00001-3

[9] Aitken RJ, Chaudhry MQ, Boxall ABA, Hull M. Manufacture and use of nanomaterials: current status in the UK and global trends. Occup Med 2006;56(5):300–6.

[10] Best JP, Dunstan DE. Nanotechnology for photolytic hydrogen production: colloidal anodic oxidation. Int J Hydrogen Energy 2009;34(18):7562–78.

[11] Hanemann T, Szabo DV. Polymer-nanoparticle composites: from synthesis to modern applications. Materials 2010; 3:3468–517.

[12] Nazari A, Riahi S, Shamekhi SF, Khademno A. Mechanical perspectives of cement mortar with Al2O3 nanoparticles. J Am Sci 2010;94.

[13] Tsai YZ, Wang NF, Tseng MR, Hsu FH. Transparent conducting Al and Y codoped ZnO thin film deposited by DC sputtering. Mater Chem Phys 2010;123(1):300–3.

[14] Gupta MK, Sinha N, Singh BK, Kumar B. Synthesis of K-doped p-type ZnO nanorods along (100) for ferroelectric and dielectric applications. Mater Lett 2010;64(16):1825–8.

[15] Elliott DW, Lien HL, Zhang WX. Degradation of lindane by zero-valent iron nanoparticles. J Environ Eng 2009;135(5):317–24.

[16] Chan J, Menon JP, Mahajan R, Jandial R. In vivo imaging of cellular transplants. Adv Exp Med Biol 2010; 671:1–12.

[17] Ratnasamy C, Wagner J. Water gas shift catalysis. Catal Rev Sci Eng 2009;51(3):325–440.

[18] Jamkhande, P. G., Ghule, N. W., Bamer, A. H., &Kalaskar, M. G. (2019). Metal nanoparticles synthesis: An overview on methods of preparation, advantages and disadvantages, and applications. Journal of Drug Delivery Science and Technology, 53. ISSN 1773-2247

[19] Klaine SJ, Alvarez PJJ, Batley GE, Fernandes TF, Handy RD, Lyon DY, et al. Nanomaterials in the environment: behavior, fate, bioavailability, and effects. Environ Toxicol Chem 2008;27(9):1825–51.

[20] Pelley AJ, Tufenkji N. Effect of particle size and natural organic matter on the migration of nano and microscale latex particles in saturated porous media. J Colloid Interface Sci 2008;321(1):74–83.

[21] F. Fan, Y. Feng, P. Tang, D.Q. Li, Facile synthesis and photocatalytic performance of ZnO nanoparticles self-assembled spherical aggregates, Mater. Lett. 158 (2015) 290–294.

[22] R. Suntako, Effect of synthesized ZnO nanograins using a precipitation method for the enhanced cushion rubber properties, Mater. Lett. 158 (2015) 399–402.

[23] E. Manikandan, L. Krishnakumar, K. Gnanasekaran,G.K. Mani, Effective Ammonia Detection Using n-ZnO p-NiO Heterostructured Nanofibers., Mater. Lett. 158 (2015) 373–376.

[24] R.K. Sonker, B.C Yadav, Growth mechanism of hexagonal ZnO nanocrystals and their sensing application., Mater. Lett. 152 (2015) 189–191.

[25] G. Hao, H. Wang, X. Li, Novel double pore structures of TiAl produced by powder metallurgy processinget al., Mater. Lett. 142 (2015) 11-14.

[26] F.T. Thema, E. Manikandan, M.S. Dhlamini, M. Maaza, Green synthesis of ZnO nanoparticles via Agathosma betulina natural extract., J. Alloy. Compd. 646 (2015) 1043–1048.

[27] N. Thovhogi, A. Diallo, A. Gurib-Fakim, M. Malik. Nanoparticles green synthesis by Hibiscus Sabdariffa flower extract: Main physical properties., J. Alloys and Compd. 647 (2015) 392–396.

[28] P. Jamdagni, P. KhatriJ, .S.Rana, Green synthesis of zinc oxide nanoparticles using flower extract of Nyctanthes arbor-tristis and their antifungal activity, Journal of King Saud University – Science, 30(2) 168-175 (2018).

[29] M. Aulice Scibioh, B.V. (2020). Chapter 3- Electrode materials for supercapacitors In materials for supercapacitor applications, pp35-204.

[30] P.C. Nethravathi, G.S. Shruthi, D. Suresh, H. Udayabhanu Nagabhushana, S.C.Sharma, Garcinia xanthochymus mediated green synthesis of ZnO nanoparticles: photoluminescence, photocatalytic and antioxidant activitystudies, Ceram. Int. 41 (2015) 8680–8687.

[31] K. Elumalai, S. Velmurugan, S. Ravi, V. Kathiravan, S. Ashokkumar, Greensynthesis of zinc oxide nanoparticles using Moringa oleifera leaf extract andevaluation of its antimicrobial activity, Spectrochim. Acta A Mol. Biomol.Spectrosc. 143 (2015) 158–164.

[32] K.A. Elsayed, N.S. Anad, G.A. Fattah, T.S. Imam, L.Z. Ismail, ZnO nanostructures induced by microwave plasma, Arab. J. Chem. 8 (2015) 553–559.

[33] A.A. Al-Owais, Synthesis and magnetic properties of hexagonally packed ZnO nanorods, Arab. J. Chem. 6 (2013) 229–234.

[34] F.T. Thema, P. Beukes, A. Gurib-Fakim, M. Maaza, Green synthesis of Monteponite CdO nanoparticles by Agathosma betulina natural extract, J. Alloys Compd. 646 (2015) 1043–1048.

[35] N. Thovhogi, A. Diallo, A. Gurib-Fakim, M. Maaza, Nanoparticles green synthesis by Hibiscus Sabdariffa flower extract: main physical properties, J. Alloys Compd. 647 (2015) 392–396.

[36] A. Diallo, A.C. Beye, T.B. Doyle, E. Park, M. Maaza, Green synthesis of Co3O4 nanoparticles via Aspalathus linearis: physical properties, Green Chem. Lett. Rev. 8 (2015) 30–36.

[37] B.T. Sone, E. Manikandan, A. Gurib-Fakim, M. Maaza, Sm 2 O 3 nanoparticles green synthesis via Callistemon viminalis' extract, J. Alloys Compd. 650 (2015) 357–362.

[38] F.T. Thema, E. Manikandan, A. Gurib-Fakim, M. Maaza, Single phase Bunsenite NiO nanoparticles green synthesis by Agathosma betulina natural extract, J. Alloys Compd. 657 (2016) 655–661.

[39] N. Thovhogi, E. Park, E. Manikandan, M. Maaza, A. Gurib-Fakim, Physical properties of CdO nanoparticles synthesised by green chemistry via Hibiscus Sabdariffa flower extract, J. Alloys Compd. 655 (2016) 314–320.

[40] Sánchez, J &Criado, Juan & Sánchez, César & Sandoval, Luis. (2009). Sanchez et al. 2009 CRIBA.

[41] S.Gaillet, J.Max. Rouanet, Silver nanoparticles: Their potential toxic effects after oral exposure and underlying mechanisms – A review, Food and Chemical Toxicology, 77, (2015), 58-63.

[42] Ramesh Chand Kasana, Nav Raten Panwar, Uday Burman, Chandra Bhushan Pandey and Praveen Kumar. 2017. Isolation and Identification of Two Potassium Solubilizing Fungi from Arid Soil. Int.J.Curr.Microbiol.App.Sci. 6(3): 1752-1762. doi: https://doi.org/10.20546/ijcmas.2017.603.201

[43] J. C. Tarafdar, Ayon Tarafdar, Wei-Ning Wang, Pratim Biswas, Green synthesis of TiO2 nanoparticle using Aspergillus tubingensis, Advanced Science, Engineering and Medicine Vol. 5, pp. 1–7, 2013.

[44] Dong J, Carpinone PL, Pyrgiotakis G, Demokritou P, Moudgil BM. Synthesis of Precision Gold Nanoparticles Using Turkevich Method. Kona. 2020 Jan 10; 37:224-232. doi: 10.14356/kona.2020011. Epub 2020 Feb 29. PMID: 32153313; PMCID: PMC7062369

[45] M. Jin, H. Zhang, Z. Xie, and Y. Xia, "Palladium nanocrystals enclosed by {100} and {111} facets in controlled proportions and their catalytic activities for formic acid oxidation," Energy Environ. Sci., vol. 5, no. 4, pp. 6352–6357, 2012.

[46] J. Turkevich, P. C. Stevenson, and J. Hillier, "The Formation Of Colloidal Gold," J. Phys. Chem., vol. 57, no. 6318, pp. 670–673, 1953.

[47] M. Brust, M. Walker, D. Bethell, D. J. Schiffrin, and R. Whyman, "Synthesis of Thiol-derivatised Gold Nanoparticles in," J. Chem. Soc. Chem. Commun., no. 7, pp. 801–802, 1994.

[48] Kołodziejczak-Radzimska A, Jesionowski T. Zinc Oxide-From Synthesis to Application: A Review. Materials (Basel). 2014 Apr 9;7(4):2833-2881. doi: 10.3390/ma7042833. PMID: 28788596; PMCID: PMC5453364.

[49] Kołodziejczak-Radzimska A., Jesionowski T., Krysztafkiewicz A. Obtaining zinc oxide from synthetic solutions of KOH and Zn(CH3COO)2. Physicochem. Probl. Miner. Process. 2010; 44:93–102.

[50] Hong R., Pan T., Qian J., Li H. Synthesis and surface modification of ZnO nanoparticles. Chem. Eng. J. 2006; 119:71–81.

[51] Kumari, Vijaya & Mittal, Anuj & Jindal, Jitender & Yadav, Suprabha& Kumar, Naveen. (2019). S-, N- and C-doped ZnO as semiconductor photocatalysts: A review. Frontiers of Materials Science. 13. 10.1007/s11706-019-0453-4.

[52] Ahmed, S. A. (2017). Structural, optical, and magnetic properties of Mn-doped ZnO samples. Results in physics, 7, 604-610

[53] Rochman, N. T., &Akwalia, P. R. (2017, May). Fabrication and characterization of Zinc Oxide (ZnO) nanoparticle by sol-gel method. In Journal of Physics: Conference Series (Vol. 853, No. 1, p. 012041). IOP Publishing.

[54] Akintelu, S.A., Folorunso, A.S. A Review on Green Synthesis of Zinc Oxide Nanoparticles Using Plant Extracts and Its Biomedical Applications. BioNanoSci. 10, 848–863 (2020). https://doi.org/10.1007/s12668-020-00774-6

[55] Gemeay, A.H., Aboelfetoh, E.F. & El-Sharkawy, R.G. Immobilization of Green Synthesized Silver Nanoparticles onto Amino-Functionalized Silica and Their Application for Indigo Carmine Dye Removal. Water Air Soil Pollut 229, 16 (2018). https://doi.org/10.1007/s11270-017-3670-4Datta, A., Patra, C., Bharadwaj, H., Kaur,

[56] S., Dimri, N., &Khajuria, R. (2017). Green synthesis of zinc oxide nanoparticles using partheniumhysterophorus leaf extract and evaluation of their antibacterial properties. Journal of Biotechnology and Biomaterials, 7, 271-275.

[57] Sutradhar, P., &Saha, M. (2016). Green synthesis of zinc oxide nanoparticles using tomato (Lycopersiconesculentum) extract and its photovoltaic application. Journal of Experimental Nanoscience, 11(5), 314-327.

[58] Griffith, P.R. and De Haseth, J.A. (1986) Fourier Transform Infrared Spectroscopy. Chem Anal Ser Monogr Anal Chem Appl, 83.

[59] Dinnebier, R.E. and Billlinge, S.J.L. (2008) Powder Diffraction: Theory and Practice. The Royal Society of Chemistry, Cambridge.https://doi.org/10.1039/9781847558237

[60] Y. Wang, C. Zhang, S. Bi, G. Luo, Preparation of ZnO nanoparticles using the direct precipitation method in a membrane dispersion micro-structured reactor, Powder Technol. 202 (2010) 130–136, https://doi.org/10.1016/j.powtec.2010.04. 027

[61] Lee, J.-H., Ko, K.-H., & Park, B.-O. (2003). Electrical and optical properties of ZnO transparent conducting films by the sol–gel method. Journal of Crystal Growth, 247(1-2), 119–125. doi:10.1016/s0022-0248(02)01907-3

[62] Raza, Waseem; Faisal, Syed Mohammad; Owais, Mohammad; Bahnemann, D.; Muneer. M. RSC Advances, 2016, 6(82), 78335-78350.